Journal of Molecular Structure 1222 (2020) 128850

Contents lists available at ScienceDirect

Journal of Molecular Structure

journal homepage: http://www.elsevier.com/locate/molstruc

Synthesis of some new pyrazolo[5,1-c][1,2,4]triazine derivatives and computational study

Fati Yıldırım [a], Aykut Demirçalı [b, *], Aslı Öztürk Kiraz [c], Fikret Karcı [b]

[a] Pamukkale University, Denizli Technical Sciences Vocational School, Department of Chemistry and Chemical Processing Technologies, Denizli, Turkey
[b] Pamukkale University, Faculty of Science-Arts, Department of Chemistry, Denizli, Turkey
[c] Pamukkale University, Faculty of Science-Arts, Department of Physics, Denizli, Turkey

ARTICLE INFO

Article history:
Received 5 March 2020
Received in revised form
2 July 2020
Accepted 6 July 2020
Available online 22 July 2020

Keywords:
Ethyl benzoyl acetate
Azo dyestuff
Pyrazole
DFT
Electronic properties

ABSTRACT

In this study, the synthesis novel of seven new pyrazolo [5,1-c][1,2,4]triazin derivative disperse dyestuffs was reported. First, 2-arylhydrazone-3-ketiminobutyronitriles were synthesized and reacted with hydrazine hydrate to afford 5-amino-4-arylazo-3-methyl-1H-pyrazoles. The 5-amino-4-arylazo-3-methyl-1H-pyrazoles were diazotised and coupled with ethyl benzoylacetate to give ethyl pyrazolylazo benzoylacetate. The final product was heated in glacial acetic acid and seven new pyrazolo [5,1-c][1,2,4] triazine dyestuffs were synthesized. FT-IR, ^{1}H NMR and elemental analysis techniques were used to characterize synthesized dyestuffs. Density functional theory calculation methods were used for to determine the molecular geometries and spectroscopic properties of the new seven dyestuffs. The acquired results from calculations and experiments are conform each other.

1. Introduction

Pyrazoles and their substituted derivatives exhibit wide variety of biological and pharmacological activities [1–8] and also find application in photography [9,10] and as dyes [11,12]. Some pyrazoles were reported to have nonnucleoside HIV-1 reverse transcriptase inhibitory activity [3,7,8,13–16].

Azolo annulated [1,2,4]triazines can be considered as isosteres of purine bases. Due to a wide and profound biological activity [17–21], this family of heterocyclic compounds causes a growing interest of researchers working in the fields of medicinal chemistry and pharmacology. Pyrazolo [5,1-c][1,2,4]triazines are similar in structure to nucleic bases, can act as metabolites and are useful as antiviral and antitumor agents [17]. In the literature, pyrazolotriazines have been reported to have cytotoxicity against cancer cells [22,23]. Berger and coworkers reported that specific polysubstituted pyrazolo [5,1-c][1,2,4]triazines inhibit selectively B-Raf kinase activity, and are preferred for the treatment of B-Raf kinase related disorders [24]. Therefore, the development of new methods and the synthesis of newly fused 1,2,4-triazine derivatives is of great importance.

Many patents and articles in the literature identify the synthesis and dyeing characteristics of monoazo dyestuff on a heterocyclic coupling component [25–28]. There are very few studies involving monoazo dyestuff based on the pyrazolo [5,1-c][1,2,4]triazine ring. In connection with our interest in this class of compounds, our study group has reported the synthesis of some pyrazolo [5,1-c] [1,2,4]triazines [29–31]. In this article, we present the synthesis of seven new monoazo dyestuff based on the pyrazolo [5,1-c] [1,2,4] triazine ring system.

In the recent years, there has been great interest to the quantum chemical calculations especially density functional theory (DFT) methods which use to determine the properties of the molecular, optical and electronic structures of the small and big sized chemical molecules at low computational time [32–35]. In this paper, as a part of continuous studies of our research group, we synthesized new pyrazolo derivatives and characterized by elemental analyses, FT-IR, ^{1}H- NMR spectroscopic methods. Also, we studied on the estimated of the geometry optimization, the vibrational frequencies, the chemical shifts and the electronic properties of azo dyestuff because of their cytotoxic activity in medical and usage as a polyester/polyamide dye in industrial applications.

* Corresponding author.
E-mail address: ademircali@pau.edu.tr (A. Demirçalı).

https://doi.org/10.1016/j.molstruc.2020.128850
0022-2860/

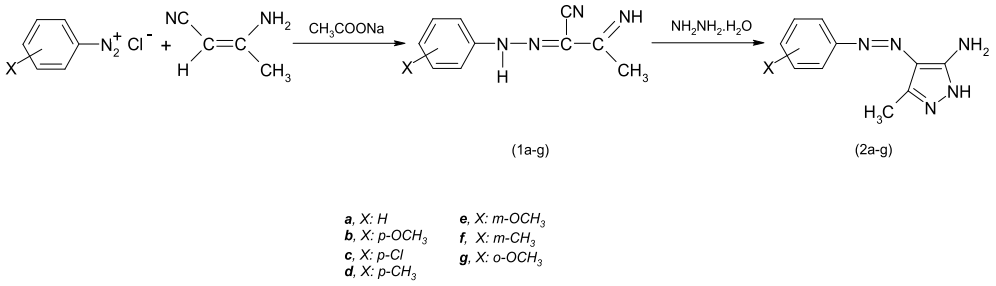

Scheme 1. Synthesis of **2a-g**.

2. Experimental

2.1. General details

The chemicals utilized in the synthesis were supplied from Aldrich and Merck Chemical Company without any purification. Suitable spectroscopic grade solvents were used.

IR spectra were recorded via PerkinElmer UATR Two (FT-IR) Spectrophotometer. ^{1}H NMR spectra were obtained on Agilent 400/55 annual refill 400 in DMSO-d_6 utilizing TMS as the internal reference and chemical shifts (δ) were reported in ppm. Melting points of dyestuffs were determined using Electrothermal 9100 melting point apparatus and not corrected.

2.2. Synthesis of 2-arylhydrazone-3-ketiminobutyronitriles (1a-g) and 5-amino-4-arylazo-3-methyl-1H-pyrazoles (2a-g)

1a-g and **2a-g** were synthesized according to the literature [36–38]**.** The general route for the synthesis of **1a-g** and **2a-g** is outlined in Scheme 1.

2.3. Synthesis of pyrazolo[5,1-c][1,2,4]triazine derivative dyestuffs (4a-g)

The synthesized 2a-g compounds (0.01 mol) were dissolved in a mixture containing glacial CH_3COOH and concentrated HCl (20 ml, ratio 1: 1), and the solution was cooled to 0–5 °C. Then $NaNO_2$ solution (0.69 g, 0.01 mol) prepared in 10 ml of water was added dropwise to this solution cooled at 0–5 °C with vigorous stirring for 1 h. The clear diazonium salt solution was added dropwise to a solution of ethyl benzoyl acetate (1.92 g, 0.01 mol) prepared in pyridine (10 ml) and cooled (0–5 °C). The pH of the coupling mixture was kept at 7–8 throughout the coupling by adding aqueous sodium acetate. Stirring was continued at 0–5 °C for 4 h and diluted with cold water (50 ml). The precipitated products were filtered, washed several times with water, dried and recrystallized from DMF-H_2O to give ethyl pyrazolylazo benzoylacetate (3a). The obtained product (3a) was refluxed for 4 h in glacial CH_3COOH (30 ml). The solvent casted out and the final product was collected by filtration and dried. It was recrystallized from DMF-H_2O (3:1) and orange crystals of the 4a dyestuff were obtained. This procedure was also used to synthesis dyestuffs 4b-g (Scheme 2). Elemental analyzes and melting points of the dyestuffs obtained are listed in Table 1.

2.4. Computational details

Quantum chemical calculations were performed at the B3LYP levels of theory with the Gaussian 16, Rev. B01 package [39] and GaussView 6.0.16 [40] was used for visualization of the structure.

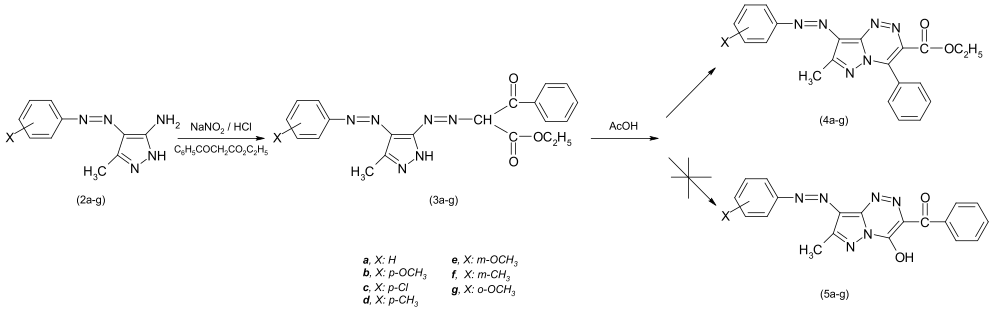

Scheme 2. Synthesis of pyrazolo [5,1-c][1,2,4]triazine derivative dyestuffs **(4a-g).**

Table 1
Elemental analysis of dyestuffs **4a-g.**

Dye no	Molecular formula (m. Wt)	m.p.[a] (°C) (colour)	Yield (%)	Elemental analysis: calc. (found)		
				C	H	N
4a	$C_{21}H_{18}N_6O_2$ (386.4)	189-191 (orange)	87	65.27 (62.65)	4.70 (4.51)	21.75 (21.37)
4b	$C_{22}H_{20}N_6O_3$ (416.4)	241-242 (red)	78	63.45 (63.86)	4.84 (4.54)	20.18 (20.47)
4c	$C_{21}H_{17}ClN_6O_2$ (420.9)	224-226 (brown)	81	59.92 (59.36)	4.07 (4.93)	19.97 (19.57)
4d	$C_{22}H_{20}N_6O_2$ (400.4)	226-227 (orange)	73	65.98 (65.53)	5.04 (5.02)	20.99 (20.68)
4e	$C_{22}H_{20}N_6O_3$ (416.4)	282-283 (orange)	84	63.45 (63.56)	4.84 (4.64)	20.18 (20.17)
4f	$C_{22}H_{20}N_6O_2$ (400.4)	281-282 (orange)	68	65.98 (59.53)	5.04 (5.02)	20.99 (20.78)
4g	$C_{22}H_{20}N_6O_3$ (416.4)	204-206 (dark red)	76	63.45 (63.66)	4.84 (4.74)	20.18 (20.27)

[a] Recrystallization from DMF/H_2O.

Geometries were optimized to the global minima at the *ab initio* DFT level 6-31G (d,p) basis set. The optimized structures were used for the calculations of vibrational frequencies, NMR chemical shift, electronic absorption spectrum and Natural Bond Orbital (NBO) analysis. We have calculated the chemical shifts of them in the ground state to differentiate the basis from the experimental chemical shifts and geometric parameters by using DFT (B3LYP) method. And also, time-dependent density functional theory (TD-DFT) was used to examine the electronic absorption spectrum. These calculations are worthy for ensuring comprehend the chemical shifts and molecular parameters.

3. Results and discussion

3.1. Molecular geometry

The geometric structures of the 4a-g compounds obtained from B3LYP/6-31G (d,p) methods are represented in Fig. 1 along with the atom numbering schemes. The 4a molecule has got 47 atoms and their basic vibrational modes are 138. The 4b, 4e and 4g molecules have got 51 atoms and their basic vibration modes are 147. While 4 and 4f molecules have got 50 atom and 114 basic vibration modes, 4c molecule has got 47 atoms and 137 basic vibration modes. The

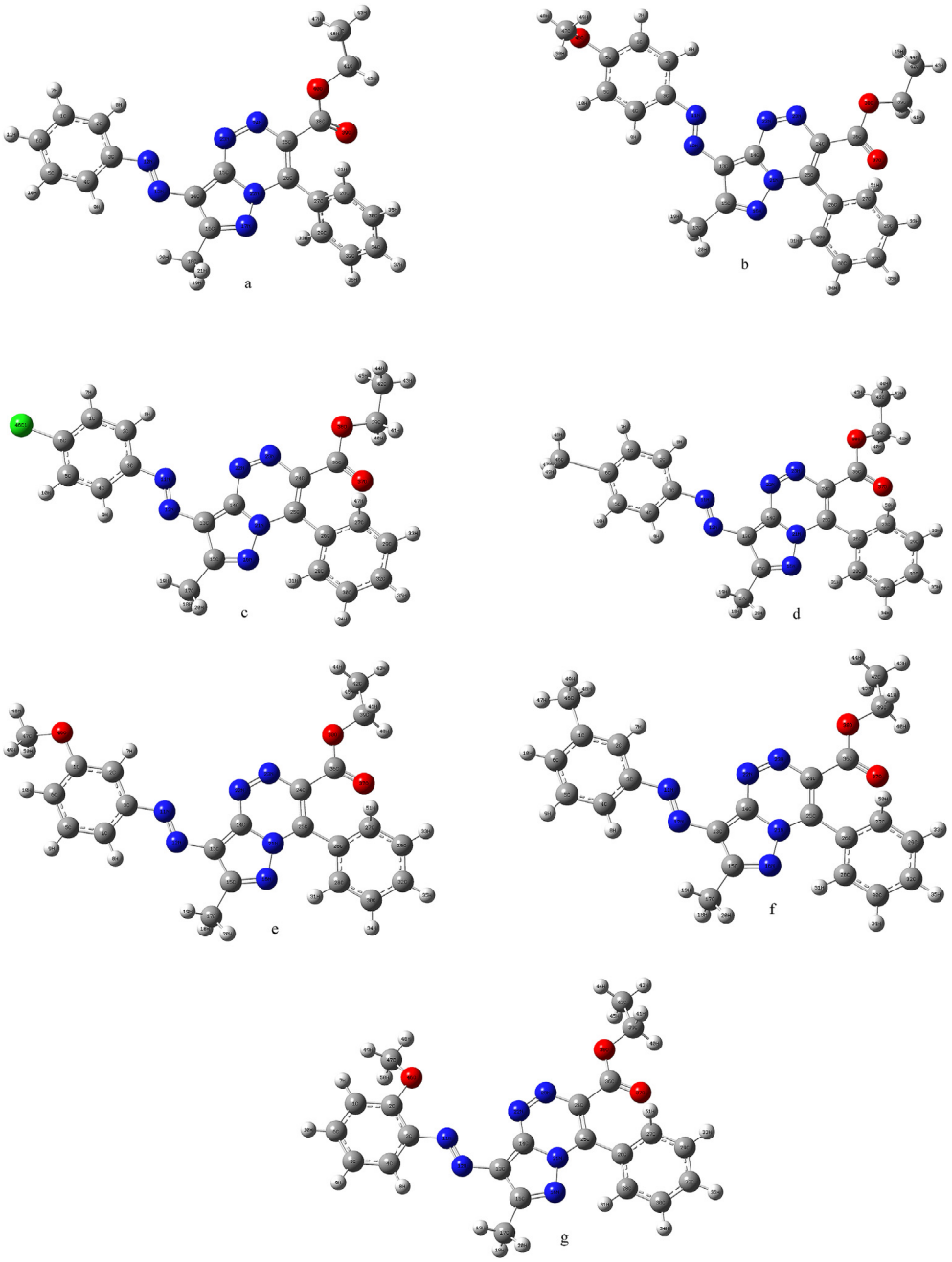

Fig. 1. The calculated optimized structure of dyestuffs **4a-g.**

Table 2
FT-IR data for dyestuffs **4a-g.**

Dye No	Vibratioanal frequencies (cm^{-1})									
	Experimental					B3LYP/6-31G (d,p)				
	ν_{Ar-H}	ν_{Al-H}	$\nu_{N=N}$	$\nu_{C=O}$	ν_{C-O}	ν_{Ar-H}	ν_{Al-H}	$\nu_{N=N}$	$\nu_{C=O}$	ν_{C-O}
4a	3062	2977	1548	1727	1022	3178	3045	1508	1800	1029
4b	3054	2977	1579	1714	1016	3207	3058	1505	1798	994
4c	3097	2987	1516	1721	1086	3186	3059	1527	1801	1055
4d	3057	2996	1564	1727	1028	3183	3038	1551	1799	1057
4e	3075	2976	1561	1726	1027	3185	3059	1598	1799	1056
4f	3061	2973	1561	1728	1029	3186	3059	1597	1799	1057
4g	3051	2982	1560	1725	1014	3184	3016	1595	1798	1058

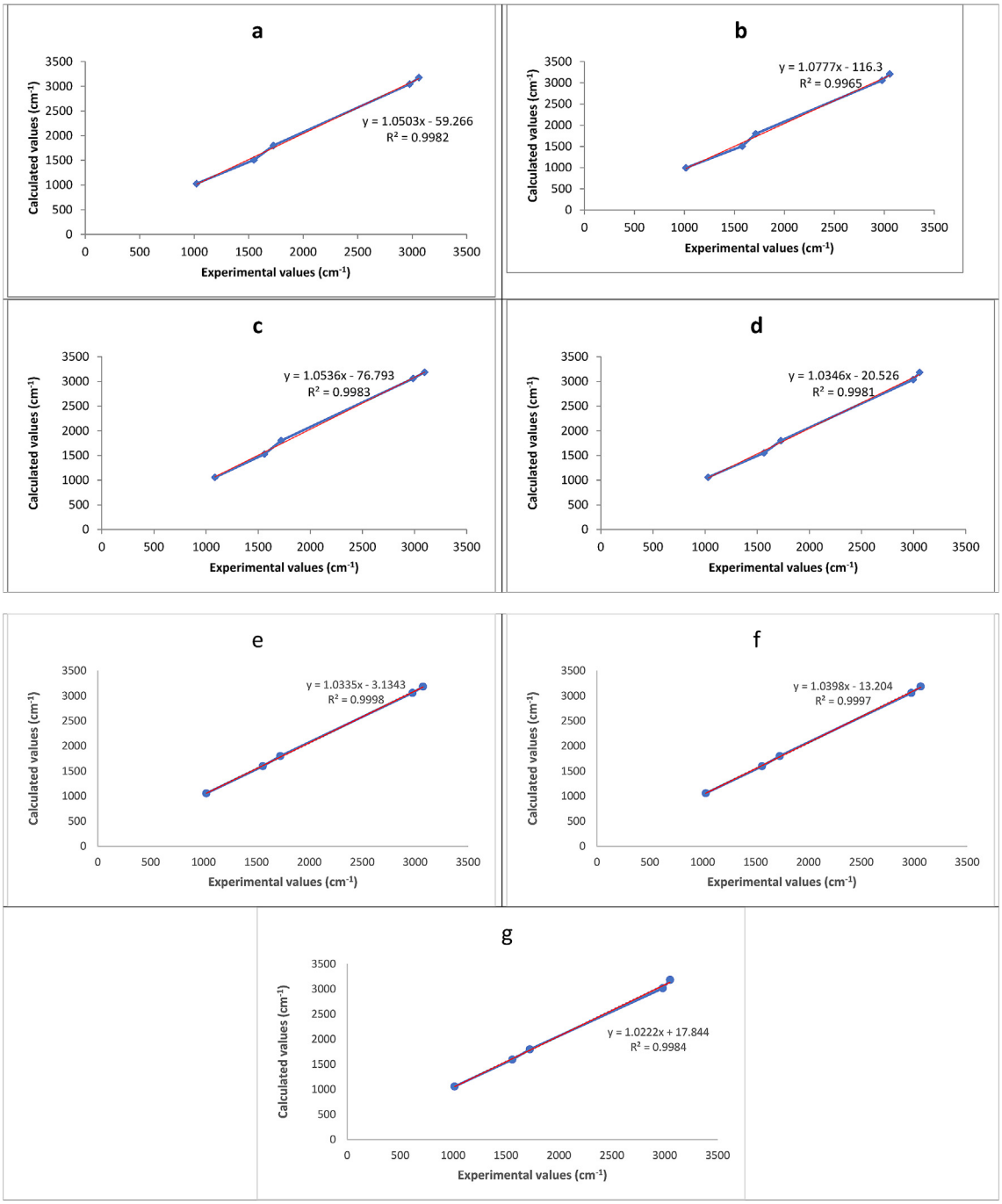

Fig. 2. Linear regression results obtained by theoretical and experimental infrared values of **4a-g** compounds.

Table 3
^{1}H NMR data for dyestuffs **4a-g.**

Dye No	^{1}H NMR[a] (δ, ppm, DMSO-d_6)			
	Experimental		B3LYP/6-31G (d,p)	
	Aro-H	Alip-H	Aro-H	Alip-H
4a	7.93–7.54 (m, 10 H)	0.99 (t, 3H, ethoxy CH_3) 2.74 (s, 3H, pyrazole CH_3) 4.18 (q, 2H, OCH_2)	8.33–7.61 (m, 10 H)	1.51 (t, 3H, ethoxy CH_3) 2.90 (s, 3H, pyrazole CH_3) 4.43 (q, 2H, OCH_2)
4b	7.13 (d, 2 H) 7.69–7.6 (m, 5 H) 7.90 (d, 2 H)	0.99 (t, 3H, ethoxy CH_3) 2.69 (s, 3H, pyrazole CH_3) 3.86 (s, $p-OCH_3$) 4.17 (q, 2H, OCH_2)	7.18 (d, 2 H) 8-49-7.72 (m, 5 H) 8.23 (d, 2 H)	1.38 (t, 3H, ethoxy CH_3) 2.85 (s, 3H, pyrazole CH_3) 3.96 (s, $p-OCH_3$) 4.29 (q, 2H, OCH_2)
4c	7.61 (d, 2 H) 7.69–7.65 (m, 5 H) 7.94 (d, 2 H)	0.99 (t, 3H, ethoxy CH_3) 2.72 (s, 3H, pyrazole CH_3) 4.18 (q, 2H, OCH_2)	7.63 (d, 2 H) 8.26–7.61 (m, 5 H) 8.22 (d, 2 H)	1.51 (t, 3H, ethoxy CH_3) 2.88 (s, 3H, pyrazole CH_3) 4.44 (q, 2H, OCH_2)
4d	7.39 (d, 2 H) 7.68–7.62 (m, 5 H) 7.81 (d, 2 H)	1.00 (t, 3H, ethoxy CH_3) 2.39 (s, $p-CH_3$) 2.69 (s, 3H, pyrazole CH_3) 4.17 (q, 2H, OCH_2)	7.62 (d, 2 H) 8.24–7.60 (m, 5 H) 8.16 (d, 2 H)	1.51 (t, 3H, ethoxy CH_3) 2.42 (s, $p-CH_3$) 2.88 (s, 3H, pyrazole CH_3) 4.43 (q, 2H, OCH_2)
4e	7.70–7.10 (m, 9 H)	0.99 (t, 3H, ethoxy CH_3) 2.69 (s, 3H, pyrazole CH_3) 3.86 (s, $m-OCH_3$) 4.17 (q, 2H, OCH_2)	8.48–7.49 (m, 9 H)	1.40 (t, 3H, ethoxy CH_3) 2.87 (s, 3H, pyrazole CH_3) 3.96 (s, $m-OCH_3$) 4.35 (q, 2H, OCH_2)
4f	7.69–7.35 (m, 9 H)	0.99 (t, 3H, ethoxy CH_3) 2.43 (s, $m-CH_3$) 2.69 (s, 3H, pyrazole CH_3) 4.17 (q, 2H, OCH_2)	8.84–7.92 (m, 9 H)	1.75 (t, 3H, ethoxy CH3) 2.85 (s, m – CH3) 3.23 (s, 3H, pyrazole CH3) 4.70 (q, 2H, OCH2)
4g	7.68–7.07 (m, 9 H)	0.99 (t, 3H, ethoxy CH_3) 2.69 (s, 3H, pyrazole CH_3) 3.97 (s, $o-CH_3$) 4.17 (q, 2H, OCH_2)	8.46–7.17 (m, 9 H)	1.41 (t, 3H, ethoxy CH_3) 2.86 (s, 3H, pyrazole CH_3) 4.14 (s, $o-CH_3$) 4.35 (q, 2H, OCH_2)

[a]Abbreviations: s, singlet, m, multiplet, d, dublet, q, quartet.

azo double bonds (N═N), the carbonyl single bond lenghts (C–O) and the carbonyl double bond lenghts (C═O) are computed in the range of 1.304–1.267 Å, 1.338–1.341 Å and 1.215–1.214 Å, respectively.

3.2. Tautomerization

^{1}H NMR spectra of the dyestuffs showed CH_3 of ethoxy group peak at 0.99–1.00 ppm and $-OCH_2$- of ethoxy group peak at 4.17–4.18 ppm. Also, ^{1}H NMR spectra of the dyestuffs did not show any the OH group peak. FT-IR spectra of the dyestuffs also did not show any the OH group peak. These suggest that these dyestuffs in the 4a-g form and not in the 5a-g form. The structures of azo dyestuffs are thought to be as shown in Scheme 2. Furthermore, it is believed that the newly synthesized dyestuffs do not have a tautomeric structure.

3.3. Vibrational analysis

The FT –IR spectra of 4a-g dyestuffs shows aromatic C H bands at 3097-3051 cm^{-1}, aliphatic C H bands at 2996-2973 cm^{-1}, azo (N═N) bands at 1579-1516 cm^{-1}, carbonyl (C = O) bands at 1728–1714 cm^{-1} and C O bands at 1086–1014 cm^{-1}. As for corresponding B3LYP/6-31G (d,p) methods, aromatic C H bands, aliphatic C H bands, azo (N═N) bands, carbonyl (C = O) bands and C O bands have been calculated as the values in the range of 3207–3178 cm^{-1}, 3059-3016 cm^{-1}, 1598-1505 cm^{-1}, 1801-1798 cm^{-1} and 1058-994 cm^{-1}, respectively. Experimental and theoretical results are tabulated in Table 2.

The correlations values (R^2) between these experimental and theoretical data for each molecule are computed and presented in Table 2. The compound 4e has the most coherent correlation with the value of 0.9998 and 4b compound has the least coherent correlation value with the value of 0.9965 which can be seen in Fig. 2. These correlation values indicated that experimental and the theoretical data are very coherent each other.

3.4. ^{1}H NMR analysis

^{1}H NMR spectra of 4a-g dyestuffs showed at 7.94–7.07 ppm (aromatic H), 4.18–4.17 ppm (OCH_2), 2.74–2.69 ppm (pyrazole CH_3) and 1.00–0.99 (ethoxy CH_3), respectively. On the other hand, the theoretical ^{1}H NMR data (4a-g dyes) obtained from B3LYP/6-31G (d,p) method are collected in Table 3 together with the experimental data.

As for corresponding B3LYP/6-31G (d,p) methods, aromatic H peaks, OCH_2 peaks, pyrazole CH_3 peaks and ethoxy CH_3 peaks have been calculated as the values of 8.84–7.17 ppm, 4.70–4.35 ppm, 2.90–2.85 and 1.75–1.38 ppm, respectively. The compound 4a has the most coherent correlation with the value of 0.9968 and 4g compound has the least coherent correlation value with the value of 0.9912 which can be seen in Fig. 3. These correlation values indicated that experimental and the theoretical data are very coherent each other.

3.5. Electronic properties

The electronic properties of a molecule are designated with the energy of HOMO (Highest Occupied Molecular Orbital) and LUMO (Lowest Unoccupied Molecular Orbitals) molecular orbitals. Beside the electronic properties the chemical reactivity, stability, optical properties and bioactivity of a molecule also determine with these parameters [41,42]. The difference between HOMO and LUMO orbitals indicates the chemical reactivity of a molecule. If the difference is small the kinetic stability of a molecule is low so the intermolecular charge transfer is very high between the electron donor and acceptor groups. When Table 4 is examined, the lowest energy gap belongs to dyestuff **4d** with 1.06 eV. On the other hand,

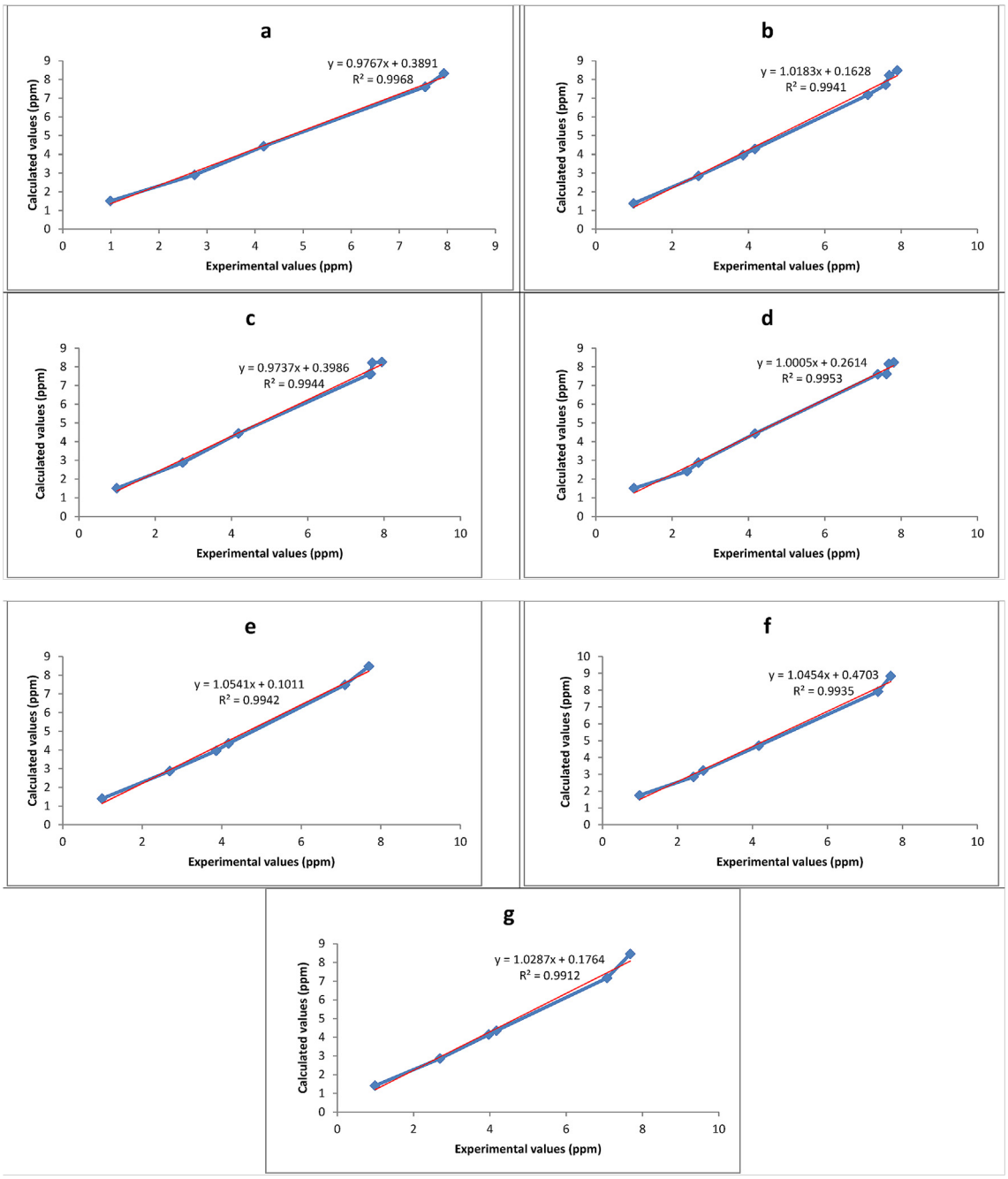

Fig. 3. Linear regression results obtained by theoretical and experimental ^{1}H NMR values of **4a-g** compounds.

Table 4
Electronic parameters of dyestuffs **4a-g**.

Parameters	4a	4b	4c	4d	4e	4f	4g
E_{HOMO} (eV)	−5.64	−5.5	−5.94	−3.67	−5.77	−5.81	−5.53
E_{LUMO} (eV)	−2.47	−2.37	−2.63	−2.61	−2.45	−2.461	−2.36
$\Delta E = E_{LUMO} - E_{HOMO}$ (eV)	3.17	3.13	3.31	**1.06**	3.32	3.35	3.17
I (eV)	5.64	5.50	5.94	3.67	5.77	5.81	5.53
A (eV)	2.46	2.37	2.63	2.61	2.45	2.46	2.36
χ (eV)	4.05	3.93	4.29	3.15	4.11	4.14	3.94
η (eV)	1.59	1.57	1.66	0.53	1.66	1.67	1.58
S (1/(eV))	0.32	0.32	0.3	0.94	0.3	0.3	0.32
μ (eV)	−4.05	−3.93	−4.29	−3.14	−4.11	−4.14	−3.94
ω (eV)	5.17	4.93	5.54	9.29	5.08	5.11	4.91

the largest energy gap belongs to dyestuff **4f** with 3.35 eV.

In compound **4d**, the $-CH_3$ group is attached to the p-position and the compound has a more linear structure. In compound **4f**, the $-CH_3$ group is attached to the meta position and is closer to the azo group containing an unpaired electron pair. The binding of the CH_3 group to the phenyl ring from different corners indicates that the meta-position dye **(4f)** may be less reactive due to the steric effect and the p-position dye **(4d)** may be more reactive due to its planar nature. The other parameters; I (ionization potential), A (electron affinity), χ (electronegativity), η (hardness), S (softness), μ (electronic chemical potential) and ω (global electrophilicity index) values of dyestuff **4a, 4b, 4c, 4e, 4f** and **4g** are nearly similar. Because of the delocalization of the conjugated πbonds, the HOMO-LUMO orbitals are located in the aromatic rings and azo groups, as seen Figs. 4 and 5.

The absorption spectra were computed using the TD-DFT method in combination with the same functional, basis set in gas phase and in chloroform. The calculated maximum absorption wavelengths (λ_{max}), and electronic transitions are shown in Table 5. The highest electronic absorption bands are calculated at 531.9 nm

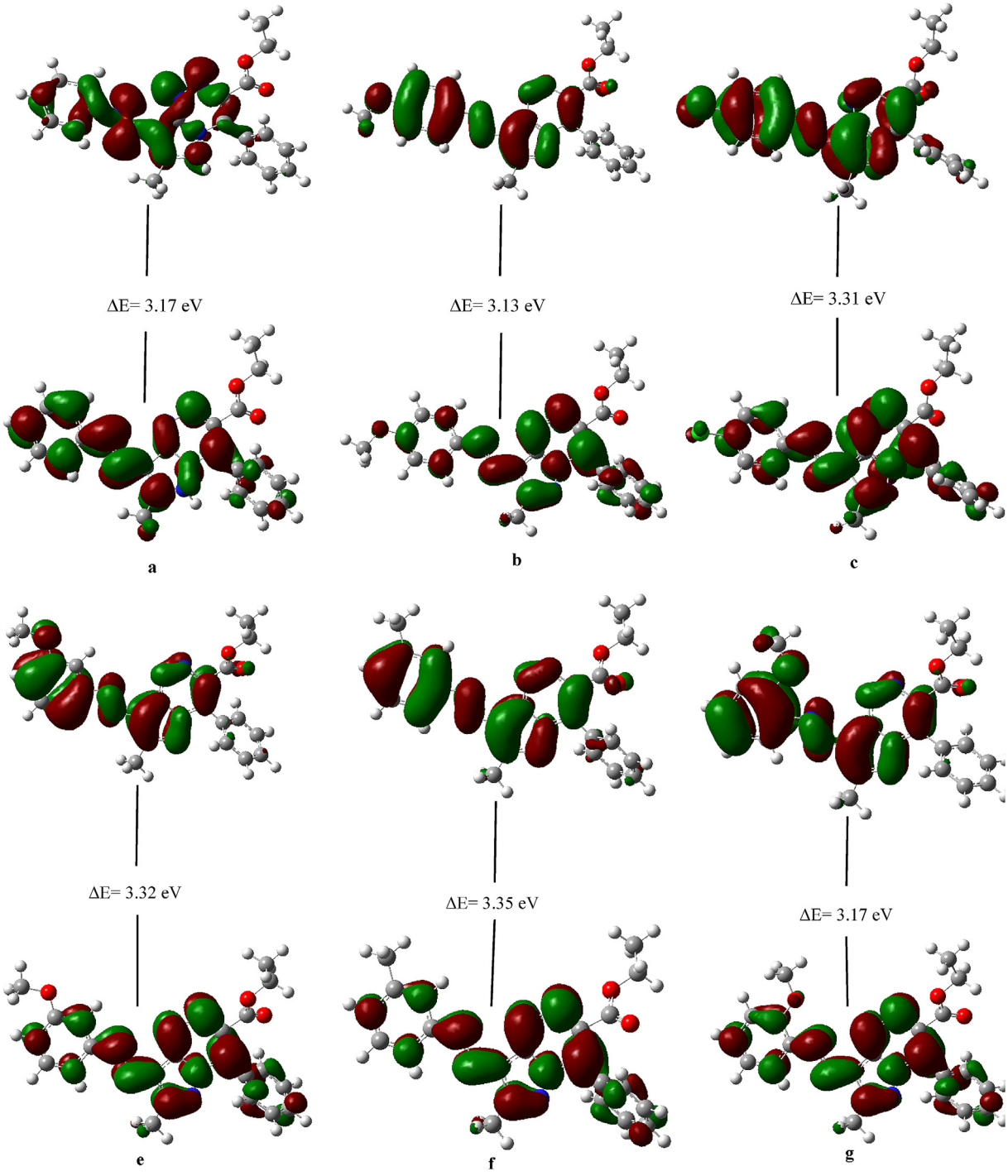

Fig. 4. HOMO-LUMO orbitals diagram of the dyestuffs **4a-g.**

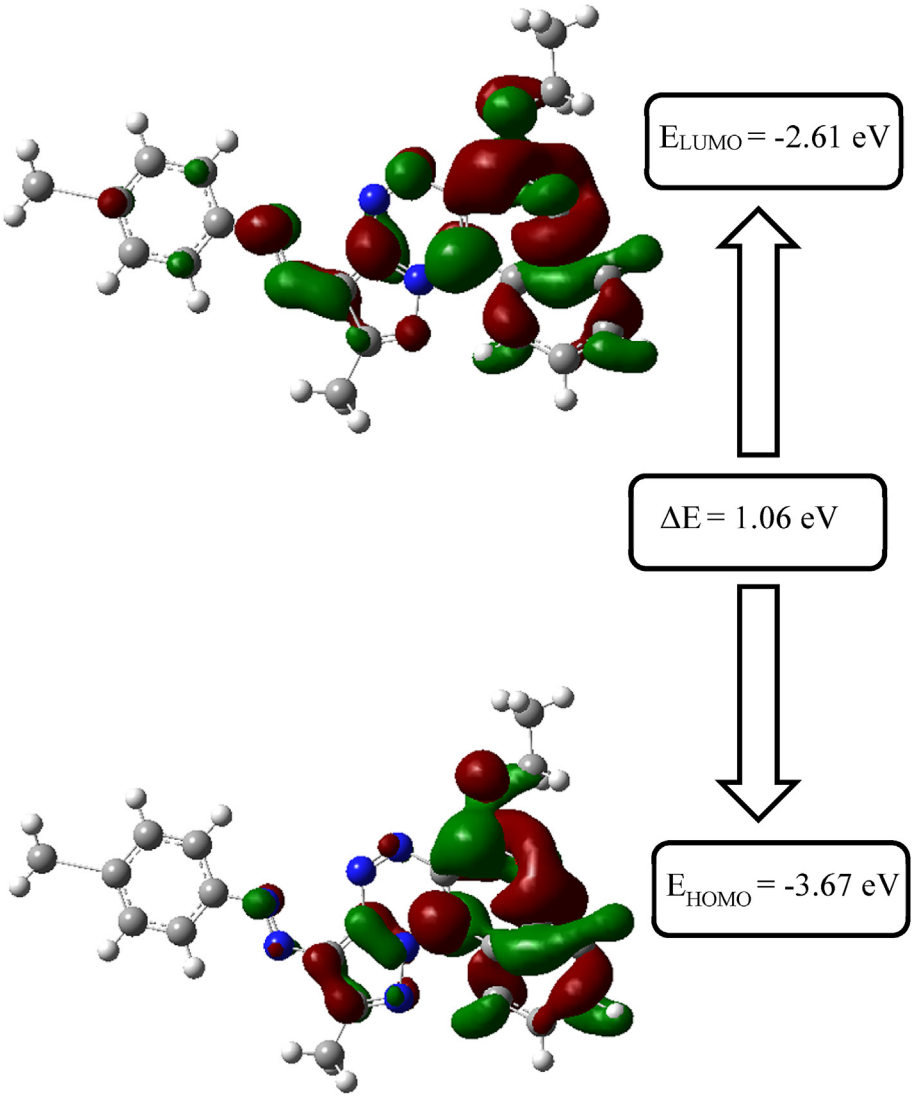

Fig. 5. Atomic composition of dyestuff **4d**.

in gas phase and 517.2 nm in chloroform by using TD-DFT/B3LYP/6-31G (d,p) level for **4g** and also they can be attributed $\pi \rightarrow \pi^*$ and $n \rightarrow \pi^*$ transitions. They were determined that these band caused by the transitions of HOMO-1 → LUMO (78%), HOMO-1 → LUMO+1 (14%), HOMO → LUMO (6%). The corresponding peaks for compounds **4a-f** in chloroform were obtained at 507.6 nm HOMO-1 → LUMO (79%), 499.1 nm with the contribution HOMO-1 → LUMO (84%), 504.7 nm with the contribution HOMO-1 → LUMO (86%), 505.6 nm with the contribution HOMO-1 → LUMO (84%), 503.2 nm with the contribution HOMO-1 → LUMO (84%) and 507.2 nm with the contribution HOMO-1 → LUMO (84%), respectively, as can be seen in Table 5. These values are also similar with the obtained from the gas phase calculations. The contribution rate of HOMO–LUMO orbitals are determined by using the GaussSum 2.2 program [43].

3.6. Natural bond orbital (NBO) analysis

Additionally, the 6-31G (d,p)/B3LYP level were performed to the natural bond orbital (NBO) calculations for the complexes **4a-g**. NBO analysis provides a favorable charge transfer or conjugation interaction in the molecular system, and also uses work on intermolecular binding and interaction between bonds [44]. The $E^{(2)}$ value computed from the NBO analysis show the energy of interaction between the electron acceptor and the electron donor and the larger value demonstrates an intense interaction between electron donors and electron acceptors [45].

As seen from Table 6, the calculated $E^{(2)}$ values presented that the significant charge flows generally occurred from the lone pair of the carbon atoms of the pyrazole ring (C13 or C14) to the π^* bond of (N22–N23) which have stabilization energy in the range of 331.89–338.67 kcal/mol. Also, electron densities given in Table 6 are another evidence of the larger electron delocalization.

4. Conclusions

Seven new pyrazolo [5,1-c][1,2,4]triazine derived azo dyestuffs have been synthesized. Characterization of these molecules was achieved by FT-IR and ^{1}H NMR spectrum measurements. Molecular structures of azo dyestuffs synthesized according to FT-IR and ^{1}H NMR results were found to be in 4a-g form. The structures, electronic and vibration properties of novel azo dyestuffs examined by density functional methods. The vibration frequencies of some of the main peaks found with the help of experimental and theoretical studies are compatible with each other and correlation values were

Table 5
Calculated absorption wavelengths, energies and oscillator strengths of **4a-g** using the TD-DFT method at the B3LYP/6- 31G (d,p) level.

	Excitation Major Contribution	CI expansion coefficient	Wavelength Calc. Gas phase (nm)	Excitation Energy (eV)	Oscillator Strength (f)	Excitation	CI expansion coefficient	Wavelength Calc. Chloroform (nm)	Excitation Energy (eV)	Oscillator Strength (f)
4a (Excited State, Singlet-A)	100 → 102 (77%) (HOMO-1→LUMO) 100 → 103 (18%) (HOMO-1→LUMO+1)	0.61988 0.29818	516.6	2.40	0.0005	100 → 102 (79%) HOMO-1→LUMO 100 → 103 (16%) HOMO-1→LUMO+1	0.62960 0.28704	507.6	2.44	0.0011
4b (Excited State, Singlet-A)	108 → 110 (82%) (HOMO-1→LUMO) 108 → 111 (15%) (HOMO-1→LUMO+1)	0.64059 0.27480	509.0	2.44	0.0000	108 → 110 (84%) HOMO-1→LUMO 108 → 111 (13%) HOMO-1 →LUMO+1 108 → 112 (2%) HOMO-1 → LUMO+2	0.64646 0.25473 0.10529	499.1	2.48	0.0003
4c (Excited State, Singlet-A)	108 → 110 (85%) (HOMO-1→LUMO) 108 → 111 (13%) (HOMO-1→LUMO+1)	0.65018 0.25328	513.1	2.42	0.0001	108 → 110 (86%) HOMO-1→LUMO 108 → 111 (10%) HOMO-1→LUMO+1	0.65761 0.22879	504.7	2.46	0.0001
4d (Excited State, Singlet-A)	104 → 106 (82%) HOMO-1→LUMO 104 → 107 (15%) HOMO-1→LUMO+1	0.63927 0.27375	514.9	2.41	0,0003	104 → 106 (84%) HOMO-1 →LUMO 104 → 107 (13%) HOMO-1→LUMO+1 104 → 108 (2%) HOMO-1 → LUMO+2	0.64695 0.25338 0.10308	505.6	2.45	0.0003
4e (Excited State, Singlet-A)	108 → 110 (78%) HOMO-1→LUMO 108 → 111 (14%) HOMO-1→LUMO+1 109 → 110 (2%) HOMO → LUMO	0.62445 0.26825 −0.1044	516.3	2.40	0.0012	108 → 110 (82%) HOMO-1 →LUMO 108 → 111 (12%) HOMO-1 →LUMO+1 109 → 110 (7%) HOMO → LUMO	0.63144 0.24723 0.18331	503.2	2.46	0.0026
4f (Excited State, Singlet-A)	104 → 106 (82%) HOMO-1→LUMO 104 → 107 (15%) HOMO-1→LUMO+1	0.63932 0.27393	517.5	2.40	0.0001	104 → 106 (84%) HOMO-1→LUMO 104 → 107 (13%) HOMO-1→LUMO+1 104 → 108 (3%) HOMO-1→LUMO+2	0.64791 0.25039 0.10286	507.2	2.44	0.0002

(*continued on next page*)

Table 5 (*continued*)

	Excitation Major Contribution	CI expansion coefficient	Wavelength Calc. Gas phase (nm)	Excitation Energy (eV)	Oscillator Strength (f)	Excitation	CI expansion coefficient	Wavelength Calc. Chloroform (nm)	Excitation Energy (eV)	Oscillator Strength (f)
4g (Excited State, Singlet-A)	108 → 110 (78%) HOMO-1→ LUMO 108 → 111 (14%) HOMO-1 → LUMO+1 109 → 110 (5%) HOMO → LUMO	0.62255 0.26681 −0.16088	531.9	2.33	0.0042	108 → 110 (78%) HOMO-1→ LUMO 108 → 111 (14%) HOMO-1→ LUMO+1 109 → 110 (6%) HOMO→ LUMO	0.62294 0.26293 −0.16931	517.2	2.40	0.0128

Table 6
Remarkable stabilization interactions in the **4a-g**.

Compound	Donor	Type	Electron Density	Acceptor	Type	Electron Density	$E^{(2)}$ (kcal/mol)
4a	C14	LP (1)	1.11080	C15−N22	π*	0.74947	331.89
	C14	LP (1)	1.11080	C16−N17	π*	0.40113	103.35
	C15−N22	π*	0.74947	N23−N24	π*	0.38591	211.87
4b	C13	LP (1)	1.09348	C14−N21	π*	0.71213	336.72
	C13	LP (1)	1.09348	C15−N16	π*	0.14742	102.61
	C14−N21	π*	0.71213	N22−N23	π*	0.38257	227.80
4c	C13	LP (1)	1.11334	C14−N21	π*	0.74506	334.13
	C13	LP (1)	1.11334	C15−N16	π*	0.39736	101.69
	C14−N21	π*	0.74506	N22−N23	π*	0.38677	217.91
4d	C13	LP (1)	1.10906	C14−N21	π*	0.75208	335.18
	C13	LP (1)	1.10906	C15−N16	π*	0.40246	103.22
	C14−N21	π*	0.75208	N22−N23	π*	0.38356	216.12
4e	C13	LP (1)	1.11067	C14−N21	π*	0.74887	331.99
	C13	LP (1)	1.11067	C15−N16	π*	0.40006	102.74
	C1−C6	π*	0.38698	C2−C3	π*	0.36498	291.78
	C1−C6	π*	0.38698	C4−C5	π*	0.29824	197.19
	C14−N21	π*	0.74887	N22−N23	π*	0.38176	213.30
4f	C13	LP (1)	1.10996	C14−N21	π*	0.75029	333.63
	C13	LP (1)	1.10996	C15−N16	π*	0.40060	102.79
	C14−N21	π*	0.75029	N22−N23	π*	0.38265	214.98
4g	C13	LP (1)	1.10566	C14−N21	π*	0.75522	338.67
	C13	LP (1)	1.10566	C15−N16	π*	0.40342	103.35
	C1−C6	π*	0.35562	C4−C5	π*	0.31224	266.34
	C2−C3	π*	0.44492	C4−C5	π*	0.31224	195.87

obtained between 0.9965 and 0.9998. The ^{1}H NMR data obtained by experimental and theoretical studies are also compatible with each other and their correlation values ranged from 0.9968 to 0.9912.

Author Contribution Statement

Fati Yıldırım: Methodology, Experimental studies, Reviewing, Analysis interpretation, Data Curation and Writing. Aykut Demirçalı: Methodology, Experimental studies, Reviewing, Analysis interpretation, Data Curation and Writing. Aslı Öztürk Kiraz: Theoretical studies, Reviewing, Analysis interpretation, Data Curation and Writting. Fikret Karcı: Review, Consultancy

Declaration of competing interest

The authors declare that they have no known competing financial interests or personal relationships that could have appeared to influence the work reported in this paper.

Acknowledgment

This study has been supported by Pamukkale University Scientific Research Project Coordination Unit by the project numbers: 2012BSP004, 2016 HZDP 036 and 2018FEBE002.

References

[1] E.C. Taylor, K.S. Hartke, The reaction of malononitrile with substituted hydrazines: new routes to 4-Aminopyrazolo[3,4-d]pyrimidines, J. Am. Chem. Soc. 81 (10) (1959) 2456−2464.
[2] A.I. Rutavichyus, S.P. Valyulene, V.V. Mozolis, J. Org. Chem. USSR (1987) 1083.
[3] S.P. Singh, D. Kumar, Reinvestigation of the reported synthesis of naphtho [2',1'-4,5]thiazolo[2,3-c][1,2,4]triazepines, Heterocycles 31 (5) (1990) 855−860.
[4] K. Langenscheid, G. Luduing, German patent (1975), 2508; Chem. Abstr., (1976) 85: 78124; Chem Abstr., (1976) 84: 44041e.
[5] E.L. Anderson, J.E. Casey, L.C. Greene, J.J. Lafferty, H.E. Reiff, Synthesis and muscle relaxant properties of 3-amino-4-arylpyrazoles, J. Med. Chem. 7 (3) (1964) 259−268.
[6] S.K. Mohant, R. Sriahar, S.Y. Padmanavan, A.A. Mittra, Indian J. Chem. 15B (1977) 146.
[7] L.H. Sternbach, The benzodiazepine story, Prog. Drug Res. 22 (1978) 66−229.
[8] N. Jaiswal, R.K. Jaiswal, J.P. Barthwal, K. Kishor, Synthesis and biological activity of some new 10-[(3,5-Diaryl-2-pyrazolin-1-yl)acetyl]-phenothiazines, Indian J. Chem. 20B (3) (1981) 252−253.
[9] D.R. David, British Patent (1977) 1491604.
[10] W. Brooker, US Patent (1953) 2646409.
[11] G. Henning, German Patent (1977) 261698.
[12] R. Jain, A. Shukla, Synthesis of some new derivatives of pyrazolin-5-ones,

J. Indian Chem. Soc. 67 (7) (1990) 575–576.
[13] Ş.G. Küçükgüzel, S. Rollas, H. Erdeniz, M. Kiraz, A.C. Ekinci, A. Vidin, Synthesis, characterization and pharmacological properties of some 4-arylhydrazono-2-pyrazoline-5-one derivatives obtained from heterocyclic amines, Eur. J. Med. Chem. 35 (2000) 761–771.
[14] L.R.S. Dias, M.J. Alvim, A.C.C. Freitas, E.J. Barreiro, A.L.P. Miranda, Synthesis and analgesic properties of 5-acyl-arylhydrazone 1-H pyrazolo [3,4-b] pyridine derivatives, Pharm. Acta Helv. 69 (3) (1994) 117–173.
[15] J.W. Lyga, R.M. Patera, M.J. Plummer, B.P. Halling, D.A. Yuhas, Synthesis, mechanism of action, and QSAR of herbicidal 3-substituted-2-aryl-4,5,6,7-tetrahydroindazoles, Pestic. Sci. 42 (1) (1994) 29–36.
[16] M.J. Genin, C. Biles, B.J. Keiser, S.M. Poppe, S.M. Swaney, W.G. Tarpley, Y. Yagi, D.L. Romero, Novel 1,5-diphenylpyrazole nonnucleoside HIV-1 reverse transcriptase inhibitors with enhanced activity versus the delavirdine-resistant P236L Mutant: lead identification and SAR of 3- and 4-substituted derivatives, J. Med. Chem. 43 (5) (2000) 1034–1040.
[17] V.L. Rusinov, E.N. Ulomskii, O.N. Chupakhin, V.N. Charushin, Azolo[5,1-c]-1,2,4-triazines as a new class of antiviral compounds, Russ. Chem. Bull. Int. Ed. 57 (5) (2008) 985–1014.
[18] G.M. Arden, D.J.W. Grant, M.W. Partridge, Action of tumour inhibitory pyrazolotriazines on klebsiella aerogenes—II: inhibition by 6-halogenoacetyl-3-methyl-4-methylenepyrazolo[3,2-c]-as-triazine and its antagonism, Biochem. Pharmacol. 19 (1) (1970) 71–89.
[19] Y.A. Ammar, N.M. Saleh, J.A. Micky, H.A.S. Abbas, M.S.A. El-Gaby, Activated nitriles in heterocyclic chemistry: facile synthesis and antimicrobial activity of some pyrimidine, pyrazolopyrimidine and pyrazolotriazine derivatives containing sulfonamido moiety, Indian J. Chem. 43B (10) (2004) 2203–2211.
[20] G. Guerrini, G. Ciciani, F. Bruni, S. Selleri, C. Guarino, F. Melani, M. Montali, S. Daniele, C. Martini, C. Ghelardini, M. Norcini, S. Ciattini, A. Costanzo, New fluoro derivatives of the pyrazolo[5,1-c][1,2,4]benzotriazine 5-oxide system: evaluation of fluorine binding properties in the benzodiazepine site on γ-aminobutyrric acid type A (GABAA) receptor. Design, synthesis, biological, and molecular modeling investigation, J. Med. Chem. 53 (21) (2010) 7532–7548.
[21] G. Guerrini, G. Ciciani, F. Bruni, S. Selleri, F. Melani, S. Daniele, C. Martini, A. Costanzo, New 3-, 8-disubstituted pyrazolo[5,1-c][1,2,4]benzotriazines useful for studying the interaction with the HBp-3 area (hydrogen bond point area) in the benzodiazepine site on the γ-aminobutyric acid type A (GABAA) receptor, Bioorg. Med. Chem. 19 (10) (2011) 3074–3085.
[22] M. Coronnello, G. Ciciani, E. Mini, G. Guerrini, B. Caciagli, S. Selleri, A. Costanzo, T. Mazzei, Cytotoxic activity of 3-nitropyrazolo[5,1-c][1,2,4]benzotriazine derivatives: a new series of anti-proliferative agents, Anti Canc. Drugs 16 (6) (2005) 645–651.
[23] G. Ciciani, M. Coronnello, G. Guerrini, S. Selleri, M. Cantore, P. Failli, E. Mini, A. Costanzo, Synthesis of new pyrazolo[5,1-c][1,2,4] benzotriazines, pyrazolo [5,1-c]pyrido[4,3-e][1,2,4] triazines and their open analogues as cytotoxic agents in normoxic and hypoxic conditions, Bioorg. Med. Chem. 16 (21) (2008) 9409–9419.
[24] D. M. Berger, M. Dh Dutia, D. W. Hopper, N. Torres, US Pat. (2009) 0082 354 Chem. Abstr. (2009) 150 374568.
[25] H. Song, K. Chen, H. Tian, Synthesis of novel dyes derived from 1-ethyl-3-cyano-6- hydroxy-4-methyl-5-amino-2-pyridone, Dyes Pigments 53 (3) (2002) 257–262.
[26] M.S. Yen, I.J. Wang, A facile syntheses and absorption characteristics of some monoazo dyes in bis-heterocyclic aromatic systems part I: syntheses of polysubstituted-5-(2-pyrido-5-yl and 5-pyrazolo-4-yl)azo-thiophene derivatives, Dyes Pigments 62 (2) (2004) 173–180.
[27] F. Karcı, A. Demirçalı, I. Şener, T. Tilki, Synthesis of 4-amino-1H-benzo[4,5] imidazo[1,2-a]pyrimidin-2-one and its disperse azo dyes. Part 1: phenylazo derivatives, Dyes Pigments 71 (2) (2006) 90–96.
[28] F. Karcı, A. Demirçalı, Synthesis of 4-amino-1H-benzo[4,5]imidazo[1,2-a] pyrimidin-2- one and its disperse azo dyes. Part 2: hetarylazo derivatives, Dyes Pigments 71 (2) (2006) 97–102.
[29] F. Karcı, İ. Şener, A. Demirçalı, N. Burukoğlu, Reactions of amino-arylazopyrazoles with active methylene compounds. Part 1: synthesis of 7-amino-3-arylazo-6-cyano-2- methylpyrazolo[5,1-c][1,2,4]triazines, Color. Technol. 122 (5) (2006) 264–269.
[30] F. Karcı, F. Karcı, Synthesis of some novel pyrazolo[5,1-c][1,2,4]triazine derivatives and investigation of their absorption spectra, Dyes Pigments 76 (1) (2008) 97–103.
[31] F. Karcı, F. Karcı, Synthesis and absorption abilities of pyrazolo[5,1-c][1,2,4] triazine based disperse dyes, Chem. Heterocycl. Compd. 49 (3) (2013) 457–465.
[32] A.K. Chandra, T. Uchimaru, The O-H bond dissociation energies of substituted phenols and proton affinities of substituted phenoxide ions: a DFT study, Int. J. Mol. Sci. 3 (2002) 407–422.
[33] A.D. Becke, Density functional thermochemistry. III. The role of exact exchange, J. Chem. Phys. 98 (7) (1993) 5648–5652.
[34] S. Sagdinc, H. Pir, Spectroscopic and DFT studies of flurbiprofen as dimer and its Cu(II) and Hg(II) complexes, Spectrochim. Acta 73 (1) (2009) 181–194.
[35] F. Ucun, A. Saglam, I. Kara, F. Karcı, Investigation of ground state tautomeric form of a heterocyclic disazo dye derived from barbituric acid by ab initio Hartree-Fock and density functional theory calculations, J. Mol. Struct. Theochem. 868 (2008) 94–100.
[36] F. Karcı, Synthesis of disazo dyes derived from heterocyclic components, Color. Technol. 121 (5) (2005) 275–280.
[37] M.H. Elnagdi, M.M.M. Sallam, H.M. Fahmy, S.A.M. Ibrahim, M.A.M. Elias, Reactions with the arylhydrazones of α c yanoketones: the structure of 2-Arylhydrazono-3-ketimino nitriles, Helv. Chim. Acta 59 (2) (1976) 55–557.
[38] M.H. Elnagdi, G.E.H. Elgemeie, F.A.E. Abd-Ellal, Recent developments in the synthesis of pyrazole derivatives, Heterocycles 23 (12) (1985) 3121–3153.
[39] M.J. Frisch, G.W. Trucks, H.B. Schlegel, G.E. Scuseria, M.A. Robb, J.R. Cheeseman, G. Scalmani, V. Barone, G.A. Petersson, H. Nakatsuji, X. Li, M. Caricato, A.V. Marenich, J. Bloino, B.G. Janesko, R. Gomperts, B. Mennucci, H.P. Hratchian, J.V. Ortiz, A.F. Izmaylov, J.L. Sonnenberg, D. Williams-Young, F. Ding, F. Lipparini, F. Egidi, J. Goings, B. Peng, A. Petrone, T. Henderson, D. Ranasinghe, V.G. Zakrzewski, J. Gao, N. Rega, G. Zheng, W. Liang, M. Hada, M. Ehara, K. Toyota, R. Fukuda, J. Hasegawa, M. Ishida, T. Nakajima, Y. Honda, O. Kitao, H. Nakai, T. Vreven, K. Throssell, J.A. Montgomery Jr., J.E. Peralta, F. Ogliaro, M.J. Bearpark, J.J. Heyd, E.N. Brothers, K.N. Kudin, V.N. Staroverov, T.A. Keith, R. Kobayashi, J. Normand, K. Raghavachari, A.P. Rendell, J.C. Burant, S.S. Iyengar, J. Tomasi, M. Cossi, J.M. Millam, M. Klene, C. Adamo, R. Cammi, J.W. Ochterski, R.L. Martin, K. Morokuma, O. Farkas, J.B. Foresman, D.J. Fox, Gaussian 16, Revision B.01, Gaussian Inc., Wallingford CT, 2016.
[40] R. Dennington, T.A. Keith, J.M. Millam, GaussView, Version 6, Shawnee Mission KS, Semichem Inc, 2016.
[41] T. Koopmans, Ordering of wave functions and eigenenergies to the individual electrons of an atom, Physica 1 (1–6) (1933) 104–113.
[42] S. Zaater, A. Bouchoucha, S. Djebbar, M. Brahimi, Structure, vibrational analysis, electronic properties and chemical reactivity of two benzoxazole derivatives: functional density theory study, J. Mol. Struct. 1123 (2016) 344–354.
[43] N.M. O'Boyle, A.L. Tenderholt, K.M. Langner, cclib: a library for package independent computational chemistry algorithms, J. Comput. Chem. 29 (2008) 839.
[44] M. Snehalatha, C. Ravikumar, I. Hubert Joe, N. Sekar, V.S. Jayakumar, Spectroscopic analysis and DFT calculations of a food additive carmoisine, Spectrochim. Acta 72A (2009) 654–662.
[45] S. Sebastin, N. Sundaraganesan, The spectroscopic (FT-IR, FT-IR gas phase, FT-Raman and UV) and NBO analysis of 4-Hydroxypiperidine by density functional method, Spectrochim. Acta 75 (2010) 941–952.